Atmospheric and oceanic evidences of El Niño-Southern Oscillation events in the south central Pacific Ocean from coral stable isotopic records over the last 137 years

Muriel Boiseau, Anne Juillet-Leclerc, Pascal Yiou, Bernard Salvat, Peter Isdale, Mireille Guillaume

PALEOCEANOGRAPHY, VOL. 13, NO. 6, PAGES 671-685, DECEMBER 1998

Atmospheric and oceanic evidences of El Niño-Southern Oscillation events in the south central Pacific Ocean from coral stable isotopic records over the last 137 years

Muriel Boiseau,[1,2] Anne Juillet-Leclerc,[1] Pascal Yiou,[1] Bernard Salvat,[3] Peter Isdale,[4] and Mireille Guillaume[5]

Abstract. We measured $\delta^{18}O$ and $\delta^{13}C$ in *Porites lutea* collected in the Moorea lagoon where the instrumental records show that an El Niño-Southern Oscillation (ENSO) event implies both a cloud cover decrease and a weak sea surface temperature (SST) increase. Two proxies allow an ENSO record to be reconstructed at Moorea: the annual $\delta^{13}C$ anomaly, associated with the South Pacific Convergence Zone motion, and an annual $\delta^{18}O$ anomaly showing increased SST. The frequency bands exhibited by the singular spectral analysis (SSA) and the multitaper method of the annual $\delta^{18}O$ and $\delta^{13}C$ records are centered on 2.5 and 5.2 years and 2.4 and 3.2 years, respectively, which are the main ENSO modes. We used SSA to reconstruct ENSO events at Moorea over the past 137 years. Results indicate that climate variability at this site is strongly affected by ENSO events.

1. Introduction

On the interannual timescale the El Niño-Southern Oscillation (ENSO) phenomenon generates most of the variability observed in global climate. ENSO induces temperature and precipitation anomalies throughout the equatorial and tropical Pacific Ocean.

Coral records are very well suited for the accuracy and timescale needed for ENSO reconstruction. Temperature is incorporated in the coral aragonite oxygen isotopic composition with a precision of ~0.5°C [*Wellington et al.*, 1996; *Leder et al.*, 1996] and a resolution of less than a month [*Gagan et al.*, 1994]. Since massive scleractinian hermatypic corals, such as *Porites*, have a life span of many centuries they are used to reconstruct the occurrence of the past ENSO events. Indeed, oxygen isotopic analyses record temperature anomalies associated with ENSO [*Dunbar et al.*, 1994] but also the dilution effect on $\delta^{18}O$ of water implied by high precipitation [*Cole and Fairbanks*, 1990].

It is important to understand the spatial and temporal evolution of ENSO events across the Pacific Ocean. While some isotopic records are available along the equatorial Pacific Ocean, nothing is known about ENSO development in the south central Pacific Ocean. In this study, $\delta^{18}O$ and $\delta^{13}C$ analyses of a core from a massive head of *Porites lutea*, collected in the Moorea lagoon (17°30'S, 149°50'W; French Polynesia), extending over the 1853-1989 period (137 years), with a bimonthly average resolution, indicate the occurrence of ENSO in the south central Pacific Ocean. During an ENSO event, meteorological measurements at Tahiti clearly show that sea surface temperature (SST) increases no more than 1°C. Although this anomaly is small, superimposed over an annual sea surface temperature amplitude of 2.3°C, the $\delta^{18}O$ signal is marked by a slight decrease. In this region, ENSO is also characterized by reduced cloudiness during the period of higher solar radiation. Since $\delta^{13}C$ records solar irradiation fluctuations, we show that ENSO events are also marked by a higher annual $\delta^{13}C$. We identified an ENSO event by an anomaly both from annual $\delta^{18}O$ and $\delta^{13}C$ records: $\delta^{18}O$ is an oceanic tracer, and $\delta^{13}C$ represents an atmospheric indicator, showing that the cloudiness anomaly always precedes the thermal anomaly. While Moorea is not located in a region associated with major ENSO anomalies, none the less, $\delta^{18}O$ and $\delta^{13}C$ records are very sensitive to large climatic changes, enabling the ENSO propagation across the south Pacific Ocean to be examined over the last 137 years.

2. Environmental Setting of the Study Area

2.1. Meteorological Parameters

No local environmental data are available from Moorea (Figure 1). Since Tahiti is very close to Moorea (25 km) we used the climatic records from the meteorological station at

[1]Laboratoire des Sciences du Climat et de l'Environnement, Laboratoire mixte CNRS-CEA, Gif-sur-Yvette Cedex, France.
[2]Now at Institute of Geophysics and Planetary Physics, University of California, Los Angeles, California.
[3]Laboratoire de Biologie Marine, EPHE, URA-CNRS 1453, Université de Perpignan, Perpignan Cedex, France.
[4]Australian Institute of Marine Science, PMB n°3, Townsville, Queensland, Australia.
[5]Laboratoire de Biologie des Invertébrés Marins, Museum National d'Histoire Naturelle, Paris, France.

Paper number 98PA02502.
0883-8305/98/98PA-02502$12.00

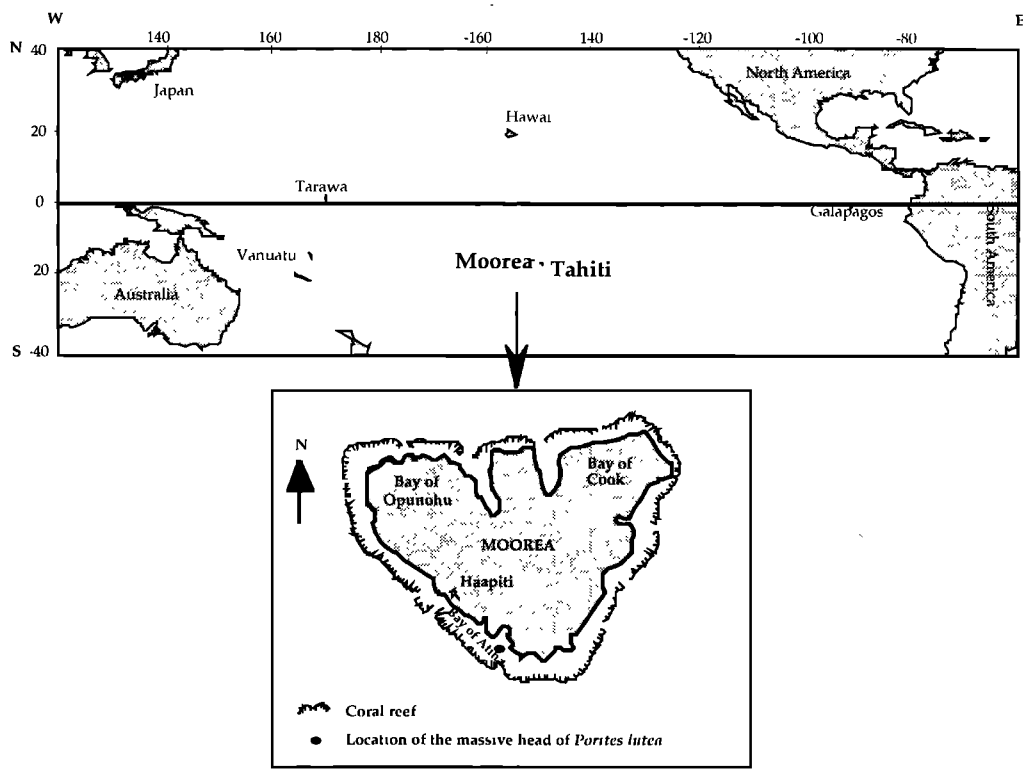

Figure 1. Map of the Pacific Ocean showing the position of Moorea (17°30'S, 149°50'W) and the location of the coral collection site on Moorea, in front of the district of Haapiti in the Atiha Bay

Faaa, where daily rainfall, insolation, cloud cover, and air temperature have been carefully measured since the 1960s.

2.1.1. Air temperature. Monthly air temperature record was compiled from 1958 to 1990 to derive an annual composite curve (Figure 2), which was calculated by averaging the monthly air temperatures over the period 1958-1990. From November, trade winds blow from the northeast, bringing warm, moist air over Moorea; the mean annual maximum air temperature, 27.1 (± 0.6, 1σ, and n = 33)°C, occurs in March. From May, the air temperature decreases because of trade wind activity, which comes from the southeast, bringing dry, cool air; the mean annual minimum, 24.4 (± 0.5, 1σ, and n = 33)°C, occurs in August. The mean annual amplitude is small, 2.8 (± 0.5, 1σ, and n = 33)°C.

2.1.2. Sea surface temperature. Monthly SSTs were measured by Institut Français de Recherche Scientifique pour le Développement en Coopération (ORSTOM) in the Tahiti backreef area from 1979 to 1990. Considering the good agreement between air temperature and SST signals, for each month we calculated the positive discrepancy between SST and air temperature. We deduced an annual composite curve of the difference between SST and air temperature. For each month of the air temperature record extending over the 1958-1990 period we added the mean monthly temperature of this annual composite curve to the monthly air temperature. The relationship between the calculated SST and the measured SST, over the 1979-1990 period, shows a high correlation coefficient (r = 0.82 and n = 144): each SST variation is correctly expressed in the reconstructed SST signal. By averaging monthly SST over the 1958-1990 period we obtained an annual composite curve of this SST record (Figure 2).

During the austral summer the South Equatorial Countercurrent brings warm seawater to the Society Islands, and the mean annual maximum SST in March is 27.8 (± 0.6, 1σ, and n = 33)°C. On the other hand, during the austral winter, influenced by the southeast trades, cool seawater is brought by the South Equatorial Current, and the mean annual minimum SST, 25.5 (± 0.5, 1σ, and n = 33)°C, occurs in August. The annual amplitude of averaged SST is 2.3 (± 0.5, 1σ, and n = 33)°C over the 1958-1990 period.

2.1.3. Rainfall - sea surface salinity. The backreef zone where the coral core was collected can be considered a relatively confined environment (Figure 1). The seawater salinity in this area is influenced by the changes in the rainfall/evaporation balance. The seasonal distribution of rainfall depends on the strong seasonal variability in position and in the intensity of the South Pacific Convergence Zone (SPCZ).

By averaging monthly precipitation over the 33 years we obtained a composite record of the annual rainfall (Figure 2). At the beginning of the austral winter the SPCZ is poorly developed. Precipitation is low, ~65 mm month^{-1} from May to September. The mean annual minimum precipitation is 44 (± 35, 1σ, and n = 33) mm and occurs in August. On the other hand, during the austral summer the SPCZ moves southwestward and is well developed, bringing abundant precipitation with ~202 mm month^{-1} from October to April. The mean annual maximum rainfall, occurring in January, is 314 (± 237, 1σ, and n = 33) mm

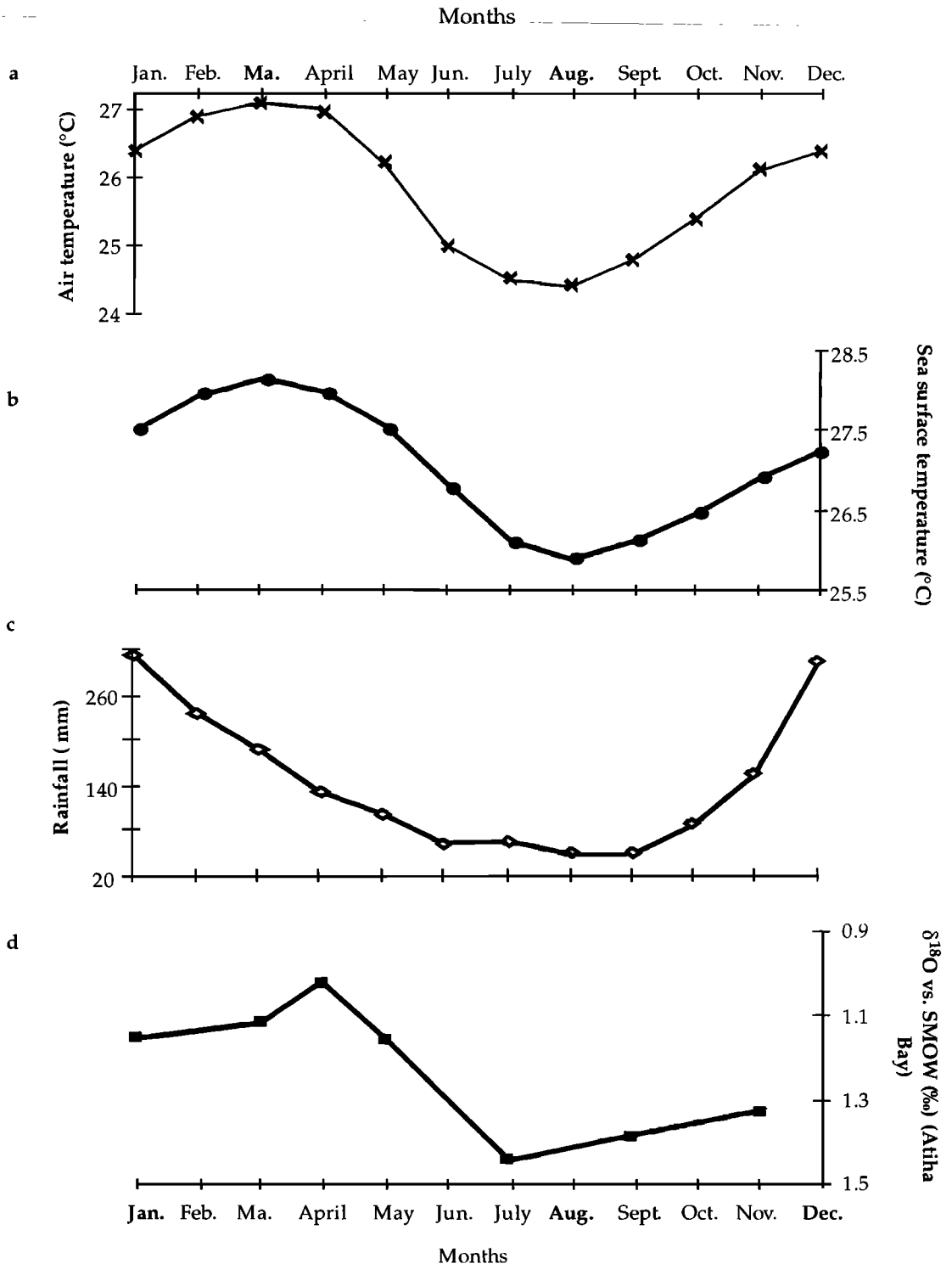

Figure 2. Composite annual curves calculated by averaging (a) monthly air temperatures, (b) reconstructed monthly sea surface temperatures (SSTs) and (c) monthly rainfall from 1958 to 1990 and (d) measurements of $\delta^{18}O_{seawater}$ (water samples were collected in the Atiha bay from March 1995 to April 1996).

The tidal range at Tahiti is almost negligible; seawater is essentially exchanged by the current generated by water carried over the outer barrier reef and into the lagoon [*Weber and Woodhead*, 1971]. It is the same for the Atiha Bay at Moorea (Figure 1). Consequently, we assume that the subannual fluctuations of sea surface salinity (SSS) measured in the Tahiti backreef zone by ORSTOM from 1979 to 1990 are similar to those of the Atiha Bay. Monthly average SSS ranged from 35.6

(± 0.3, 1σ and n = 12) (in March) to 36.0 (± 0.2, 1σ, and n = 12)‰ (in October). The annual amplitude of salinity is weak: 0.4 (± 0.3)‰.

2.2. ENSO Record in the Moorea Island

In order to clarify the chronology of an ENSO event occurrence we consider that the year recording the beginning of the temperature anomaly preceding the onset of an ENSO event is called the year (-1), the year (0) corresponds to the year marked by the maximal thermal anomaly along the southwest American coast, and the year (+1) is associated with the year following the warm event [*Philander*, 1989].

At Moorea, during an ENSO event as the sea level pressure decreases in the southeast tropical Pacific at the end of year (-1), the SPCZ, moving northward, is less intense, and therefore rainfall significantly weakens from January to April of year (0). Therefore contrary to the equatorial zone, the wet season in this tropical area is characterized by lower precipitation. *Rougerie et al.* [1985] observed, from meteorological records from the Faaa station and Tahiti-ORSTOM, that a decrease of rainfall implies significant reduction in cloud cover and that the insolation measurements (number of sunny hours per month) showed an anomalous increase during the wet season of year (0). During the next wet season of year (+1), rainfall was also weak, but this effect was not as significant. During an ENSO event, Moorea is also affected by temperature anomalies [*Rougerie et al.*, 1985]. However, for each ENSO event the temperature record from Faaa station exhibits an increase of ~1°C from February to April of year (+1). The SSTs stay warm during the austral winter of year (+1) and start to cool during the austral summer of year (+2).

3. Material and Sampling Methods

3.1. Material

In October 1990, a colony of *P. lutea* located on the edge of the lagoon in front of the district of Haapiti (Figure 1) was drilled at a depth of 5 m. The present study is the result of isotopic analyses of the upper 1.65 m of the coral core, which has a diameter of 7.9 cm.

The core was cut into 8 mm thick slabs oriented perpendicular to the density bands and parallel to the growth axis. Each slab was cleaned with deionized water and X rayed to reveal the pattern of density bands. On the basis of X ray negatives, subannual samples for isotopic analyses were collected by low-speed drilling, in order to avoid a mineralogical inversion from aragonite to calcite, using a 0.8 mm diameter drill. We collected an average of six discrete samples per annual band every 2 mm along the maximum growth axis.

3.2. Analytical Methods

The data are expressed in the conventional delta notation relative to a standard:

$$\delta^{13}C = [\,(^{13}C / ^{12}C)_{sample} / (^{13}C / ^{12}C)_{standard} - 1\,] \times 10^3,$$

$$\delta^{18}O = [\,(^{18}O / ^{16}O)_{sample} / (^{18}O / ^{16}O)_{standard} - 1\,] \times 10^3.$$

The standard is Peedee belemnite (PDB) for carbonate analyses and standard mean ocean water (SMOW) standard for water $\delta^{18}O$.

Boiseau and Juillet-Leclerc [1997] demonstrated that for this coral core, because of both organic matter and secondary crystallized inorganic aragonite, the isotopic shift after a H_2O_2 (30%) treatment is small but sufficient to reveal a seasonal signal both in $\delta^{13}C$ and in $\delta^{18}O$ that is not evident in the untreated subsamples. Therefore each drilled sample, 400 µg of aragonite powder, was chemically treated following the procedure described by *Boiseau and Juillet-Leclerc* [1997] before isotopic analyses.

For the isotopic analyses, 100 µg of aragonite powder were dissolved in 95% H_3PO_4 at 90°C. The resulting CO_2 gas was then analyzed with a VG Optima mass spectrometer. From 78 measurements of a carbonate standard the external mass spectrometer reproducibility is ±0.08‰ (1σ) and ±0.06‰ (1σ) for $\delta^{18}O$ and $\delta^{13}C$, respectively. From 1512 coral aragonite analyzed samples, 464 were duplicated. Thus we obtained an intrasample reproducibility combined with instrumental precision of ± 0.08‰ (1σ and n = 464) for $\delta^{18}O$ and ± 0.11‰ (1σ and n = 464) for $\delta^{13}C$.

From March 1995 to April 1996, 100 mL of seawater were collected every 2 months in the Moorea backreef zone near the colony of *P. lutea* analyzed in this study. The oxygen isotopic composition of seawater samples was analyzed with a Finnigan MAT 252 with a reproducibility of ± 0.05‰ (1σ).

4. Results and Discussion

4.1. Oxygen Isotopic Compositions From a *Porites lutea* Section

$\delta^{18}O$ measurements ranged from -4.80‰ to -3.41‰ (Figure 3a) and revealed seasonal variations.

4.1.1. Chronology. Since the pattern of density bands at the top of this coral core is unclear the seasonality of the intra-annual $\delta^{18}O_{aragonite}$ was used to establish a precise chronology. However, the $\delta^{18}O_{aragonite}$ signal depends on both SST variations and the seasonal oscillations of the seawater isotopic composition ($\delta^{18}O_{water}$), which vary simultaneously. Hence we estimated which of these two climatic parameters is predominant in the $\delta^{18}O_{aragonite}$ variability.

The relative distribution of rainfall and SST versus time (Figure 4) compared with $\delta^{18}O$ versus core depth over the 1979-1990 period emphasizes a strong similarity between SST and $\delta^{18}O$. Consequently, the $\delta^{18}O$ cyclicity reflects essentially temperature oscillations according to the studies of *Leder et al.* [1996] and *Wellington et al.* [1996]. The chronology is then established by associating each maximum and minimum in $\delta^{18}O$ with each minimum (August) and maximum (March) in the SST record (Figure 2), assuming a constant linear extension rate between these 2 months. The skeletal oxygen isotopic composition shows a mean annual amplitude of 0.48 (± 0.18)‰ over the 1853-1989 period.

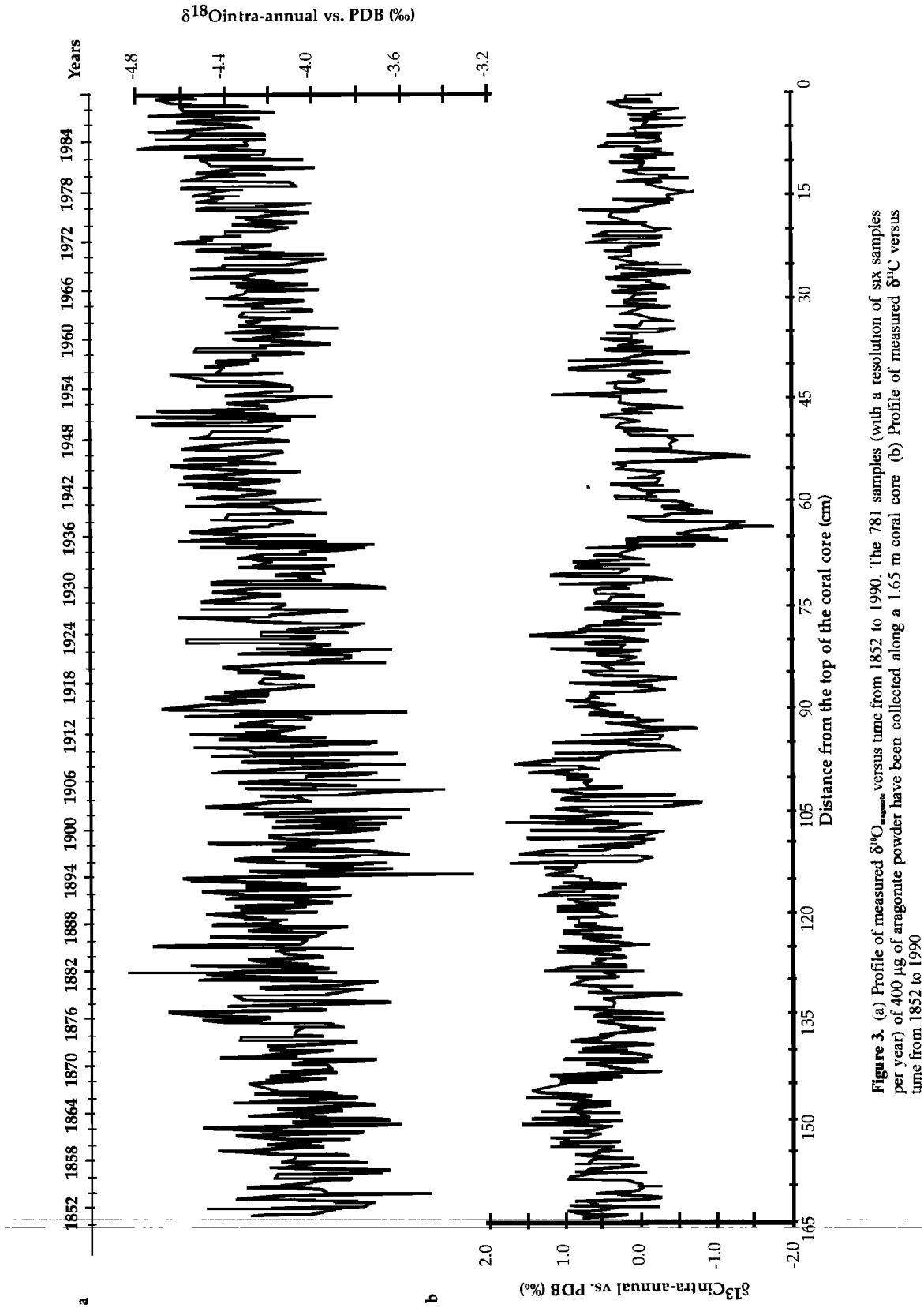

Figure 3. (a) Profile of measured $\delta^{18}O_{aragonite}$ versus time from 1852 to 1990. The 781 samples (with a resolution of six samples per year) of 400 μg of aragonite powder have been collected along a 1.65 m coral core (b) Profile of measured $\delta^{13}C$ versus time from 1852 to 1990

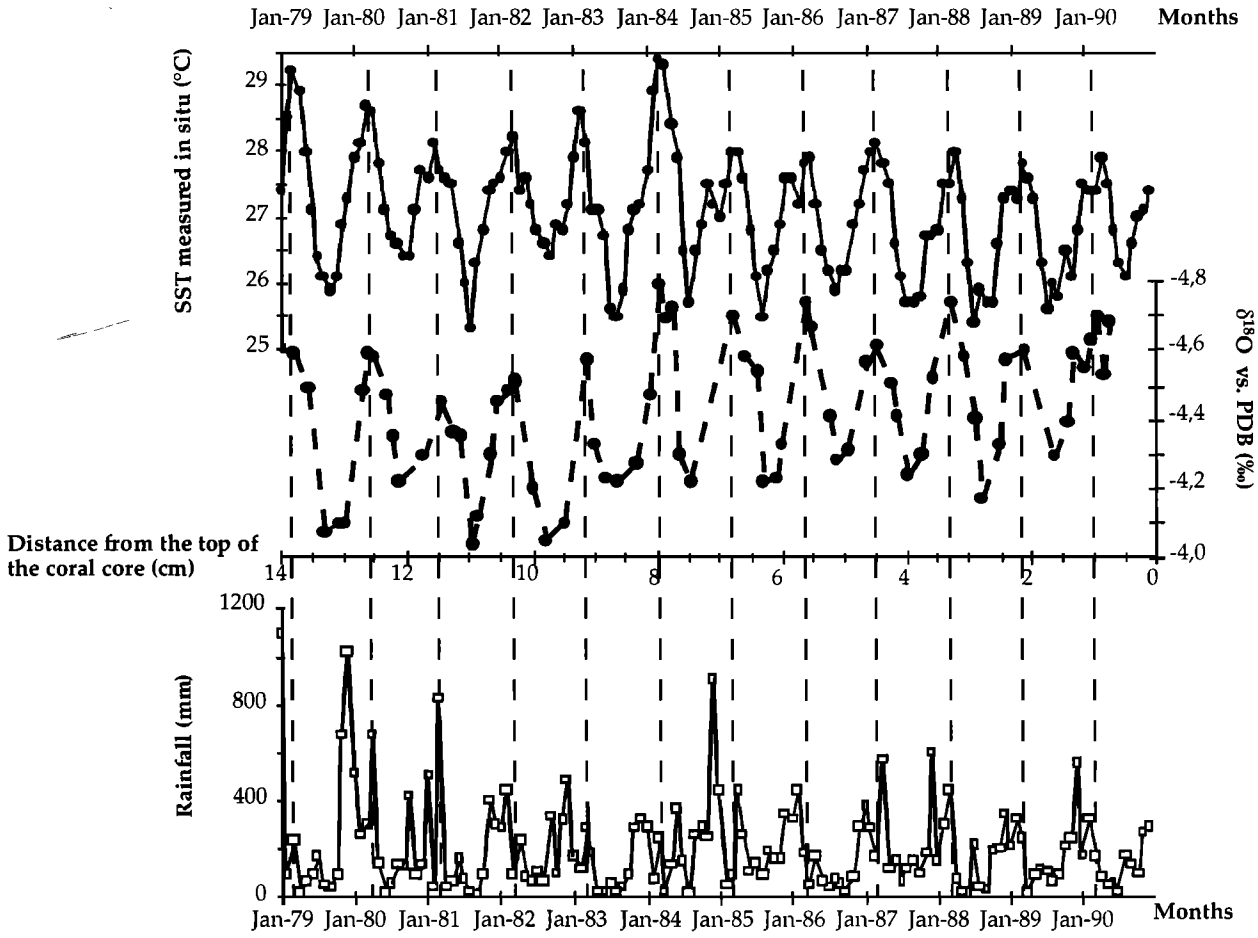

Figure 4. Profiles of SST, measured in situ by Institut Français de Recherche Scientifique pour le développement en Coopération, rainfall, measured at the Faaa station, and the intra-annual $\delta^{18}O$ versus time from 1979 to 1990. The $\delta^{18}O$ oscillations show a better fit with SST than with precipitation variations.

4.1.2. Comparisons between intra-annual variations of SST and $\delta^{18}O_{aragonite}$. The record of SST is only available over a very short period (1979-1990). From the isotopic chronology each measured $\delta^{18}O$ is associated with a clear date (month-year), and each of these dates (month-year) corresponds to a SST value. Therefore we calculate an intra-annual relationship between SST and $\delta^{18}O$ over the 1979-1990 period (Table 1, equation (1)). Equation (1) is statistically significant to 90% according to a Student distribution. Since the chronology is based on the association of each $\delta^{18}O$ minimum or maximum with each SST minimum or maximum we verified that the SST-$\delta^{18}O$ relationship remains statistically significant without considering the extreme values of $\delta^{18}O$ and SST (Table 1, equation (2)). Correlation (2) shows that the isotopic chronology adopted for this study seems to be correct and that the assumption that the extension rate is constant between March and August and August and March for each year does not seem so bad.

Monthly air temperature was available over the 1958-1990 period. We calculated a monthly SST signal from measurements taken in situ for both air and sea surface temperatures. We calculated over the period 1979-1990 the relationship between $\delta^{18}O$ and assessed intra-annual SST values both by considering March and August $\delta^{18}O$ and SST (Table 1, equation (3)) and without considering these extreme values (Table 1, equation (4)). The slopes for (1) and (3), and for (2) and (4) are similar taking into account the error calculated for each slope. Thus we used the reconstructed SST record from 1958 to 1990 to calibrate the oxygen isotopic data. The SST-$\delta^{18}O$ relationship over the 1958-1990 period is also statistically significant to 90% according to a Student distribution (Table 1, equation (5)).

However, the slope of the SST-$\delta^{18}O$ calibrations in (5), like the others (Table 1), is lower than that previously published from monthly measurements of $\delta^{18}O$ and SST, perhaps because variability in $\delta^{18}O_{water}$ was not considered [*Quinn et al.*, 1996]. Therefore the smoothed slopes may be because of low sampling frequency [*Leder et al.*, 1996; *Wellington et al.*, 1996], metabolic effects that are not linear over the range of growth rates with respect to environmental change [*McConnaughey*, 1989], distortion of environmental signals caused by skeletogenesis mechanism [*Barnes et al.*, 1995], and the seasonal seawater isotopic composition fluctuations [*Wellington et al.*, 1996; *Leder et al.*, 1996]. Therefore we estimated the influence of these parameters on the subannual oxygen isotopic composition of coral aragonite.

Table 1. Sea Surface Temperature-$\delta^{18}O$ Regression Equations Derived From the Coral Data at Moorea.

Period	Relationship Between	Regression Equation	Degree of Freedom	R
1979-1990	intra-annual SST (measured in situ) and intra-annual $\delta^{18}O$	$\delta^{18}O$ = -0 14 (±0 04) x SST - 0 59 (1)	67	0 699
1979-1990	intra-annual SST (measured in situ) and intra-annual $\delta^{18}O$, without taking into account isotopic values corresponding to March and August	$\delta^{18}O$ = -0 12 (±0.05) x SST - 1.16 (2)	45	0 585
1979-1990	intra-annual SST (calculated from air temperature record) and intra-annual $\delta^{18}O$	$\delta^{18}O$ = -0 16 (±0 03) x SST - 0 07 (3)	67	0 801
1979-1990	intra-annual SST (calculated from air temperature record) and intra-annual $\delta^{18}O$, without taking into account isotopic values corresponding to March and August	$\delta^{18}O$ = -0 15 (±0 02) x SST - 0 38 (4)	45	0 703
1958-1990	intra-annual SST (calculated from air temperature record) and intra-annual $\delta^{18}O$	$\delta^{18}O$ = -0.15 (±0 02) x SST - 0 42 (5)	194	0 764
1958-1990	interannual SST (calculated from air temperature record) and interannual $\delta^{18}O$, taking into account the calendar years	$\delta^{18}O$ = -0 23 (±0 03) x SST + 1 84 (6)	31	0 755
1958-1990	interannual SST (calculated from air temperature record) and interannual $\delta^{18}O$, taking into account the climatic periods (Y-1, Y)	$\delta^{18}O$ = -0 22 (±0 07) x SST + 1 49 (7)	31	0 762

Each relationship is statistically significant to 90% according to Student distribution and the variance of the slopes is estimated from a York regression.

4.1.3. Effect of sampling resolution on the amplitude of $\delta^{18}O_{aragonite}$. The isotopic signal, which covers 137 years, is derived from 781 isotopic measurements. Hence we adopted a bimonthly averaged sampling resolution. According to *Leder et al.* [1996] and *Wellington et al.* [1996] this resolution is low, and the annual isotopic range is undoubtedly smoothed. To examine the isotopic effect of two different sampling resolutions on the coral core, knowing that a 0.8 mm drill hole roughly corresponds to 1 month deposition, we compared the isotopic profiles obtained for two consecutive years with a monthly resolution (one sample every month) and a bimonthly resolution (one sample every 2 months) (Figure 5). These two samples were taken from very close calyces. Figure 5a clearly shows that in contrast to *Leder et al.*'s [1996] finding, there appears to be no attenuation of the isotopic signal at these two different sampling regimes. We agree with the study of *Quinn et al.* [1996]: a high resolution does not always imply a greater accuracy of climate information when corals grow at sites with small annual temperature variation. Indeed, if we compare the mean annual isotopic amplitude and the annual isotopic compositions obtained from a monthly and a bimonthly sampling resolution values differ by no more than 0.10‰ and 0.09‰, respectively (Figure 5a). Taking into account the reproducibility of oxygen (± 0.08‰), these different resolutions have no sampling effect; thus the bimonthly sampling adopted in this study appears to reflect the true range of isotopic signals.

4.1.4. Influence of aragonite deposition mechanism on intra-annual $\delta^{18}O_{aragonite}$ record. We may assume that the seasonal $\delta^{18}O$ range can also be reduced by the smoothing that occurs during skeletogenesis. Indeed, calcification takes place through two successive steps: formation of a framework followed by a progressive filling in of residual intercrystalline space [*Barnes and Lough*, 1993]; the samples collected for isotopic measurements at any given depth composed of a mixture of skeletal elements accreted at different times. In this study the coral tissue layer of core *P. lutea* extends to ~6.5 mm below the outermost surface of the coral skeleton and the mean annual extension rate is 12.2 mm. The infilling could take place in 6 months and smooth the isotopic amplitude as demonstrated by *Barnes et al.* [1995] for *Porites* genus. Consequently, the aragonite deposition of coral could explain the weak slopes of the obtained SST-$\delta^{18}O$ relationships. Moreover, whatever the smoothing, the annual $\delta^{18}O$ amplitude may be reduced while the annual $\delta^{18}O$ is not affected.

4.1.5. Effect of variations in seawater isotopic composition on the $\delta^{18}O_{aragonite}$ oscillations. Since there is no runoff in the Atiha Bay the fluctuations of the $\delta^{18}O_{seawater}$ in this part of the Moorea lagoon are entirely controlled by the evaporation-rainfall balance. Bimonthly seawater samples have been collected in the backreef area where the coral core was drilled, from March 1995 to April 1996, providing only a few $\delta^{18}O_{seawater}$ measurements. From October to April the average salinity was lowest, 35.73‰, and the water was lower in ^{18}O (1.14‰) because of abundant rainfall. During the dry season the mean salinity is 35.85‰ and the mean $\delta^{18}O_{seawater}$ was 1.32‰. The $\delta^{18}O_{seawater}$ distribution is seasonal and closely influenced by rainfall variations (Figure 2). Throughout the year, seawater of the Moorea backreef area is enriched in ^{18}O (the annual average is 1.2‰) compared to the open ocean

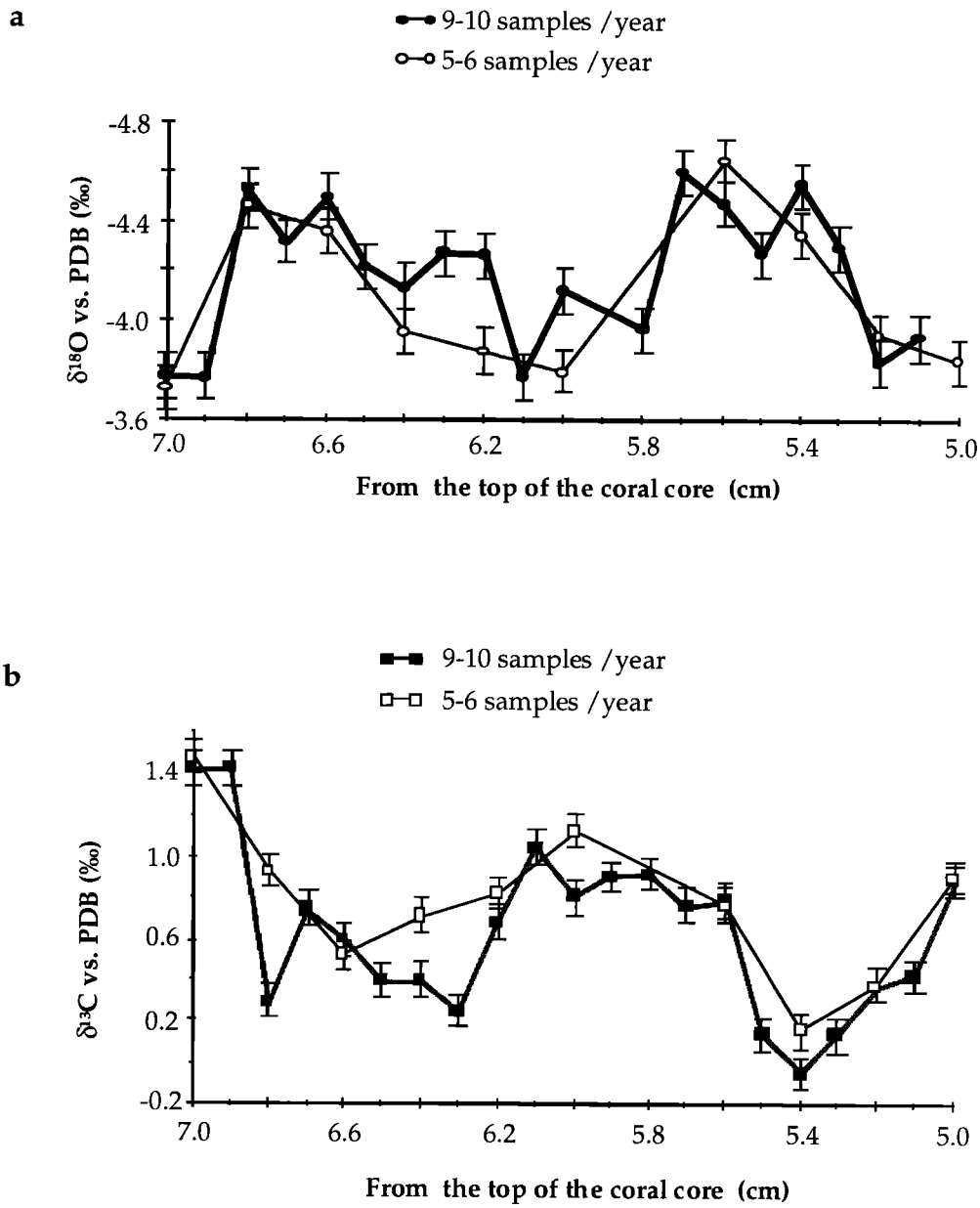

Figure 5. Comparison between a monthly and a bimonthly sampling resolution: (a) for oxygen and (b) for carbon.

(~0.7‰). The backreef zone is a semiconfined environment, where evaporation is prevailing and only a weak dilution occurs because of the seasonal rainfall.

We cannot evaluate the direct impact of $\delta^{18}O_{seawater}$ variation on $\delta^{18}O_{aragonite}$ since from 1958 to 1990 $\delta^{18}O_{seawater}$ measurements were not available. However, we deduce from $\delta^{18}O_{seawater}$ measurements that the seasonal fluctuations of the $\delta^{18}O_{seawater}$ implies an increase of the slope of the equation (5). However, over the 1958-1990 period the slope of the interannual SST-$\delta^{18}O$ calibration (Table 1, equation (6), and Figure 6), without taking into account the intra-annual $\delta^{18}O_{water}$ variability, is similar to the slopes derived from thermodynamics calculations and laboratory experiments [*Epstein et al.*, 1953; *Tarutani et al.*, 1969; *Grossman and Ku*, 1986]. This slope is also in close agreement with the values obtained for *Porites* from annual SST and $\delta^{18}O$ by both *Druffel* [1985] and *Carriquiry et al.* [1994], -0.22‰/°C, and by *McConnaughey* [1989], -0.21‰/°C. Consequently, it implies that the annual oxygen isotopic signal reflects only the annual SST fluctuations in *Porites* collected in the Atiha Bay.

4.1.6. Influence of extension rate. Some authors have suggested that skeletal growth rate and isotopic composition are inversely related [*Leder et al.*, 1996]. We estimated the annual extension rate (the distance between two successive $\delta^{18}O$ minima) and plotted $\delta^{18}O$ versus this estimation: no significant correlation links the annual growth rates to annual isotopic compositions.

In conclusion, the oxygen isotopic signal is neither biased by the annual extension rate fluctuations nor by the sampling method adopted in this study. Therefore the seawater isotopic

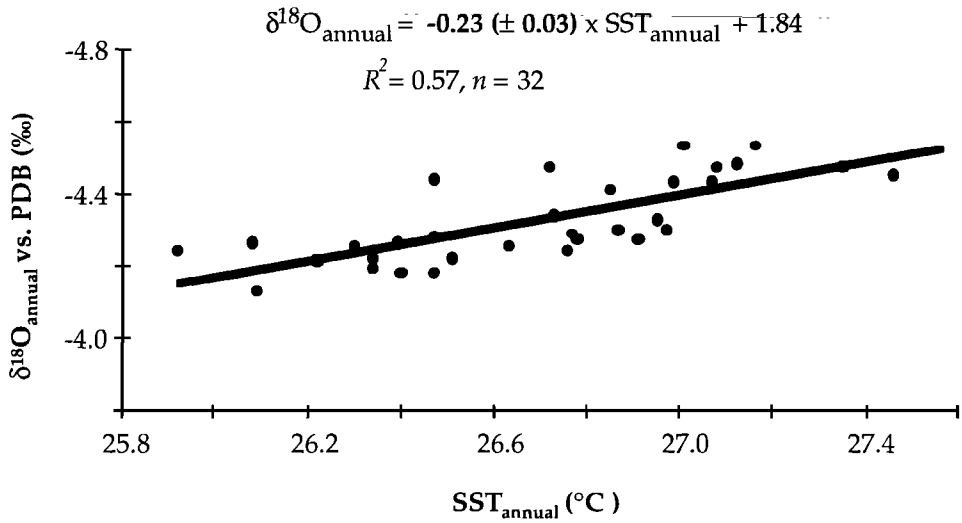

Figure 6. Relationship between the annual $\delta^{18}O$ and SST from 1958 to 1990. The SST are calculated from the air temperature recorded at the meteorological station in Tahiti

variability and the skeletogenesis mechanism could explain the slope of the equation (5). Unfortunately, these effects cannot be quantified. The annual $\delta^{18}O_{aragonite}$ from a coral core in the Atiha Bay may then be used to interpret regional changes in the interannual variations of SST.

4.2. Carbon Isotopic Composition From a *Porites lutea* Section

The intra-annual measurements of $\delta^{13}C$ also show seasonality with values ranging from -1.71 to 1.77‰ (Figure 3b). Coral aragonite is always depleted in ^{13}C relative to inorganic aragonite. Previous studies suggest that this depletion decreases when the annual extension rate is high [*McConnaughey*, 1989]; consequently, a higher annual extension rate can imply a stronger depletion in ^{13}C. By plotting annual isotopic compositions versus annual growth rates, according to *Swart et al.* [1996], no significant correlation links the growth rates to isotopic compositions. The annual extension rate does not appear to be the prevailing factor affecting annual $\delta^{13}C$ variation. The difference between the mean annual carbon isotopic amplitudes obtained from a monthly and bimonthly sampling resolution is no more than 0.11‰ (Figure 5b), and the difference between the annual isotopic composition resulting from these two resolutions is no more than 0.15‰. Taking into account the reproducibility of carbon (± 0.11‰), these different resolutions have no isotopic effect. The $\delta^{13}C$ variations from coral aragonite depend on the water-dissolved inorganic carbon (DIC) variability and metabolic processes.

4.2.1. Effect of water dissolved inorganic carbon (DIC) on $\delta^{13}C_{aragonite}$. Previous authors consider that $\delta^{13}C_{aragonite}$ may be affected by the DIC variability [*Swart et al.*, 1996]. The seasonal fluctuations can result from river runoff and the overall productivity of the reef community. In the Haapiti district, as there is no river, the seawater DIC of Atiha Bay cannot be depleted in ^{12}C because of a seasonal massive discharge of freshwater [*Swart et al.*, 1996]. Because of the photosynthetic activity, algae preferentially use ^{12}C, therefore enriching the seawater in ^{13}C. No data of seawater $\delta^{13}C$ of the Atiha Bay are available; however, high island lagoons are very poor in phytoplankton because of a frequent oligotrophy. The productivity variability is reduced; consequently, the carbon isotopic composition of seawater has a weak intra-annual fluctuation. Hence we may consider that the annual DIC fluctuation is around constant. The main effect on $\delta^{13}C$ signal is then probably caused by the metabolic fractionation driven by variations in light level.

4.2.2. Coral metabolic fractionation. Skeletogenesis takes place from an internal inorganic carbon pool This carbon reservoir is composed from bicarbonate and carbonate ions dissolved in seawater and by CO_2 resulting from metabolic processes. Photosynthetic activity of zooxanthellae may change the carbon isotopic composition of the inorganic carbon pool and consequently the $\delta^{13}C$ of coral skeleton [*Fairbanks and Dodge*, 1979; *Swart*, 1983, *Juillet-Leclerc et al.*, 1997]. According to the model of *Goreau* [1977], when the photosynthetic activity of algae is maximal, they preferentially use ^{12}C from the internal dissolved inorganic carbon pool, and thus ^{13}C essentially remains in the reservoir and is incorporated into the skeleton. Consequently, the more important the photosynthetic activity of zooxanthellae is, the more positive the $\delta^{13}C$ of the coral skeleton is.

Over the 1853-1989 period the mean annual minimum $\delta^{13}C$, -0.04 (± 0.49, 1σ)‰, occurs in April while there are two mean annual maxima $\delta^{13}C$, occurring either in December, 0.56 (± 0.50, 1σ)‰, or in August, 0.51 (± 0.50, 1σ)‰. If we admit that the $\delta^{13}C$ variability essentially reflects the metabolic activity fluctuations, we deduce that photosynthesis is more important at the end of the year (when the rainfall is at a maximum) or during the cloudless period. From visual inspection the subannual variations of $\delta^{13}C$ over the 1958-1990 period are divided into two categories: the years characterized by the highest values of $\delta^{13}C$ in August and the others characterized by the highest values of $\delta^{13}C$ in December.

For each year we calculated the annual mean of $\delta^{13}C$ and noted that when the photosynthetic activity is higher in November-January than in August, the annual mean of $\delta^{13}C$ is very large (Figure 7). On the other hand, when the photosynthetic activity is more intense in August than in

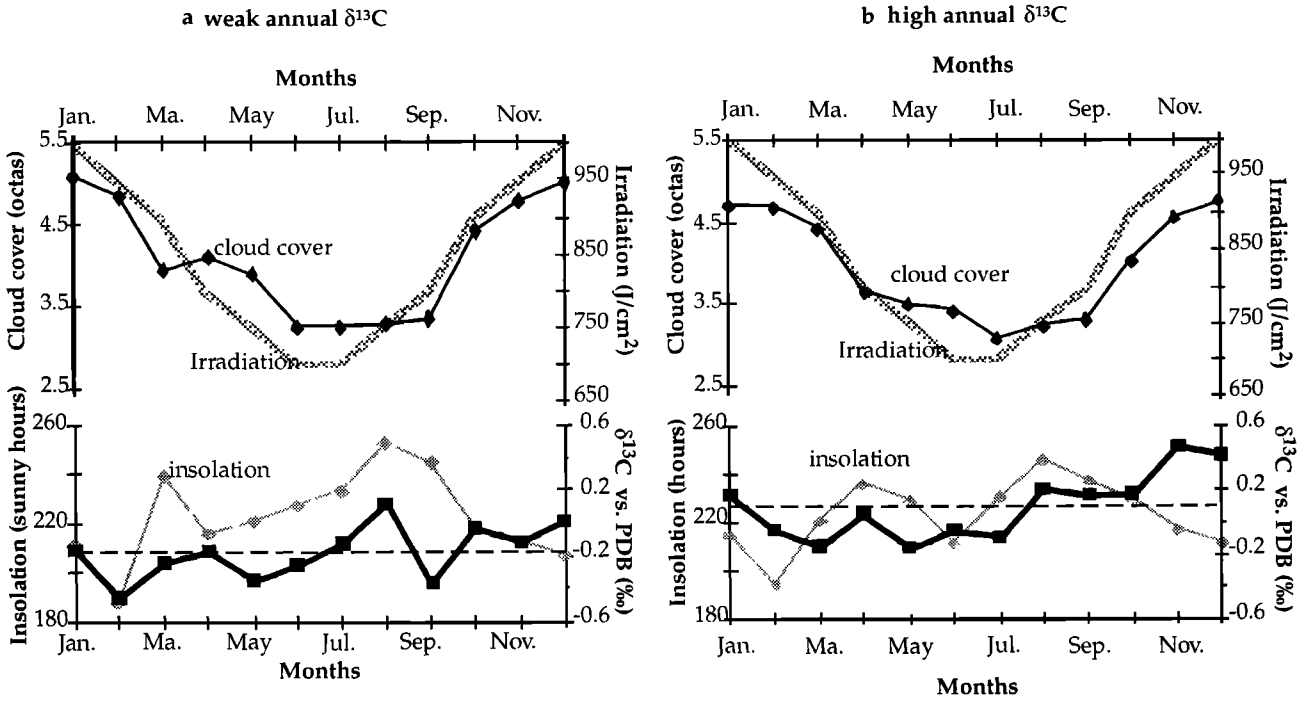

Figure 7. Comparison between years characterized by the highest $\delta^{13}C$ in August and the highest $\delta^{13}C$ in November-December. For each case we calculated an annual composite $\delta^{13}C$ curve compared to annual composite curves of cloud cover, insolation during the same years and annual solar irradiation distribution. The two annual composite $\delta^{13}C$ curves are statistically different according to the Student test. (a) When the highest $\delta^{13}C$ is recorded in August, the annual $\delta^{13}C$ is low (-0.18‰) (b) When the highest $\delta^{13}C$ occurs in November-December, the annual $\delta^{13}C$ is higher (0 10‰).

November-January, the annual $\delta^{13}C$ mean is very low We explain these two different responses of the photosynthetic activity by the variations of both irradiation (in terms of solar energy, J cm^{-2}) and insolation (number of sunny hours per month). From the insolation data collected at the Faaa station from 1958-1990 it appears that the insolation is at a maximum in August and a minimum during the cloudy season from December to February. No solar irradiation record (in terms of energy, in J cm^{-2}) was measured at Faaa, but according to *Ivanoff* [1975], the maximum of solar irradiation occurs at the latitude of Moorea from December to January, when the cloud cover is prevailing.

Following Goreau's model, the coral skeleton accreted during the period of highest photosynthetic activity is enriched in ^{13}C. Consequently, in December, because of the cloud cover, the photosynthetic activity of zooxanthellae generally remains weak despite the maximum irradiation, and the insolation is the predominant factor, but the annual mean of $\delta^{13}C$ is reduced (Figure 7). On the other hand, when the high $\delta^{13}C$ occurs in December, precipitation and cloudiness are reduced during the wet season, implying an efficient photosynthetic activity in December because of higher irradiation; according to *Kirk* [1983] the seasonal variation in photosynthetic production is essentially a response to the annual cycle of irradiance then high $\delta^{13}C_{aragonite}$ reflects low cloud cover (Figure 7). During an ENSO event, rainfall decreases at Moorea, and the corresponding annual mean $\delta^{13}C_{aragonite}$ should be high.

In conclusion, from previous studies [*Rougerie et al.*, 1985] we know that an ENSO event affects the climatology of the Moorea with both temperature and precipitation anomalies. We previously demonstrated that the interannual $\delta^{18}O$ oscillations only reflect the interannual SST. Therefore we could detect the thermal anomaly associated with an ENSO phenomenon from the annual $\delta^{18}O$ signal Moreover, *Rougerie et al.* [1985] observed that during an ENSO event the cloud cover is reduced from November to January; that is, precipitation is abnormally weak. The solar irradiation is more important than during a normal year. Consequently, the photosynthetic activity of zooxanthellae is very intense during November-January of an ENSO year, enriching the internal DIC pool in ^{13}C. In this case the mean annual $\delta^{13}C_{aragonite}$ is large. We have two proxies at our disposal to establish an ENSO reconstruction which are characterized by an anomaly from both annual $\delta^{18}O$ and $\delta^{13}C$ records.

4.3. ENSO Events Recorded in Two Isotopic Records

One of the precursors of ENSO is the northward movement of the SPCZ from October-November of the year (-1), implying the start of the rainfall decrease in the zone of the Moorea Island. The westward propagation of anomalous conditions reaches the west coast of South America between November of the year (-1) and January of the year (0) implying an increase of sea level. This abnormal warm SST is propagated poleward in

both hemispheres. The time required for a baroclinic wave to cross the Pacific basin depends on latitude; with Moorea island located at 17°30'S latitude, the temperature anomaly affects this area of the south central Pacific Ocean from July-August of the year (0), and the thermal anomaly is at a maximum in February-May of the year (+1). Consequently, at Moorea during an ENSO event the cloudiness anomaly precedes the temperature anomaly. Since we previously demonstrated that the cloud cover anomaly is reflected by a high annual mean of $\delta^{13}C$ and that the warm SST is characterized by a low annual mean of $\delta^{18}O$ we considered that each ENSO event must be necessarily characterized at first by a high annual mean of $\delta^{13}C$ followed by a low annual mean of $\delta^{18}O$.

If the thermal anomaly appears in February-May, the precipitation anomaly can appear from December to February. In order to detect with a maximum of sensitivity the ENSO events we cannot consider the calendar years. Hence we consider periods extending from July to June. We verified that over the 1958-1990 period a similar annual $\delta^{18}O$-SST relationship is obtained according to calendar year (Table 1, equation (6)) or the period extending from July to June (Table 1, equation (7)) considered. Consequently, from the annual means of oxygen and carbon isotopic compositions, calculated for the July-June period we determinated ENSO events since 1853 in the south central Pacific.

4.3.1. Spectral analyses. Previous studies have shown that climate variability in the tropical Pacific mainly responds to the annual cycle and, to a lesser degree, to the interannual periods associated with ENSO [*Rasmusson et al.*, 1990]. Partial phase locking onto the annual cycle has been shown to lead to Devil's staircase behavior [*Jin et al.*, 1994, *Tziperman et al.*, 1994], in which rational multiples of the annual frequency are excited. Spectral analysis documents the frequencies associated with nonlinear behavior.

Yiou et al. [1996] have shown the necessity of using different methods of time series analysis in order to ensure the stability of the spectral features observed in data sets and lower the risks of spurious results. Here we used two modern techniques: the singular-spectrum analysis (SSA) [*Vautard and Ghil*, 1989] and the multitaper method (MTM) [*Thomson*, 1982]. Both methods are part of the MTM-SSA toolkit of *Dettinger et al.* [1995]. SSA allows us to decompose a time series into trend, oscillating, and noise components by analyzing its covariance matrix. Tests for composite (red noise or trend plus noise) have been devised by *Allen and Smith* [1996] and can be used as confidence intervals against a noise background. MTM is a refinement of classical Fourier analysis, with optimal properties with respect to resolution and spectral leakage. We used it to compute the power spectra of the time series and the significant line frequencies above a 90% red noise background. A conservative approach to peak detection will then be to consider only those peaks which are consistent with the two methods.

We analyzed the annual $\delta^{13}C$ and $\delta^{18}O$ time series from 1853 to 1989. We investigate subharmonic frequencies (lower frequencies) of the annual cycle. The MTM and SSA spectra for $\delta^{13}C$ and $\delta^{18}O$ are shown in Figure 8. The two time series contain a trend, which can be optimally removed by SSA (and MTM). The SSA null hypotheses (to be rejected) will thus be of red noise superimposed on a trend. Both methods detect consistent and significant (above a 90% red noise percentile) variability in the 2.5 and 5.2 year periodicity bands and in the 2.4 and 3.2 year periodicity bands in the annual mean of $\delta^{18}O$ and the annual mean of $\delta^{13}C$, respectively. The two annual records clearly contain a signature of a quasi-biennial component (2.5 years), which has previously been detected in the Southern Oscillation Index (SOI) series [*Ghil and Yiou*, 1996] and in monthly averages from Comprehensive Ocean-Atmosphere Data Set (COADS) data covering the equatorial Pacific [*Rasmusson et al.*, 1990; *Jiang et al.*, 1995] In addition, they show different lower frequencies which have also been documented and attributed to ENSO behavior, from ~4 to ~7 years [*Rasmusson et al.*, 1990; *Jiang et al.*, 1995]. The two low-frequency spectral peaks in coral isotopic records at Moorea are similar to the other coral isotopic studies from the entire Pacific Ocean. Indeed, from the records obtained on a coral core from Vanuatu islands over 173 years, *Quinn et al.* [1993] essentially found 3.0, 3.6, 4.8, and 7.5 year bands, while according to the records from Galàpagos islands corals the main oscillations occur at periods of 3 3, 4.6, and 6 years over a 400 year period [*Dunbar et al.*, 1994].

4.3.2. ENSO reconstruction. From the results of spectral analyses we can infer the ENSO influence on climate variability at that location, and hence we can examine the interannual periods clearly manifest in the two isotopic records. SSA was used to separate the interannual significant oscillatory modes from the signals of annual $\delta^{18}O$ and $\delta^{13}C$, from which the trends are removed. We obtained four isotopic climatic series centered on 2.5 and 5.2 years (from the annual $\delta^{18}O$ data) and on 2 4 and 3.2 years (from the annual $\delta^{13}C$ signal). These results are presented in the Figure 9 On the basis of a high $^{13}C/^{12}C$ ratio followed by a low $^{18}O/^{16}O$ ratio from the four isotopic climatic series we recognized 36 ENSO events which have affected the climatology of the Moorea zone over the last 137 years.

This ENSO list (Table 2) is compared both to the list previously established by *Quinn* [1992] and to the El Niño identified by COADS from 1902. Seventy percent of the events listed by COADS and 65% of events recensed by *Quinn* [1992] are reflected in our ENSO reconstruction. Therefore the climatic variability in the Moorea zone is strongly affected by the ENSO phenomenon. However, ENSO not recorded in this study include the 1902, 1965, and 1972 events, which were characterized as ones of strong intensity [*Quinn*, 1992; *Cole et al.*, 1993].

Moreover, seven events are revealed in our ENSO reconstruction which are not referenced by either *Quinn* [1992] or COADS. The $\delta^{13}C$ anomalies recorded in 1881-1882, 1891-1892, 1893-1894, 1908-1909, 1920-1921, 1935-1936, and 1955-1956 correspond to strong dry periods in Australia [*Allan*, 1985], but the SOI was positive during these years; hence this precipitation anomaly is not linked with ENSO phenomenon. The low $\delta^{18}O$, associated with the $\delta^{13}C$ anomalies indicates a SST increase in 1882-1883, 1893-1894, 1894-1895, 1909-1910, 1922-1923, 1936-1937, and 1956-1957. Since the temperature increases observed at Moorea in 1882-1883, 1893-1894, 1894-1895, 1909-1910, 1921-1922, and 1956-1957 were not referenced in other ENSO studies, it probably corresponds to a local climatic signal. The temperature increase in 1936-1937 is associated with an El

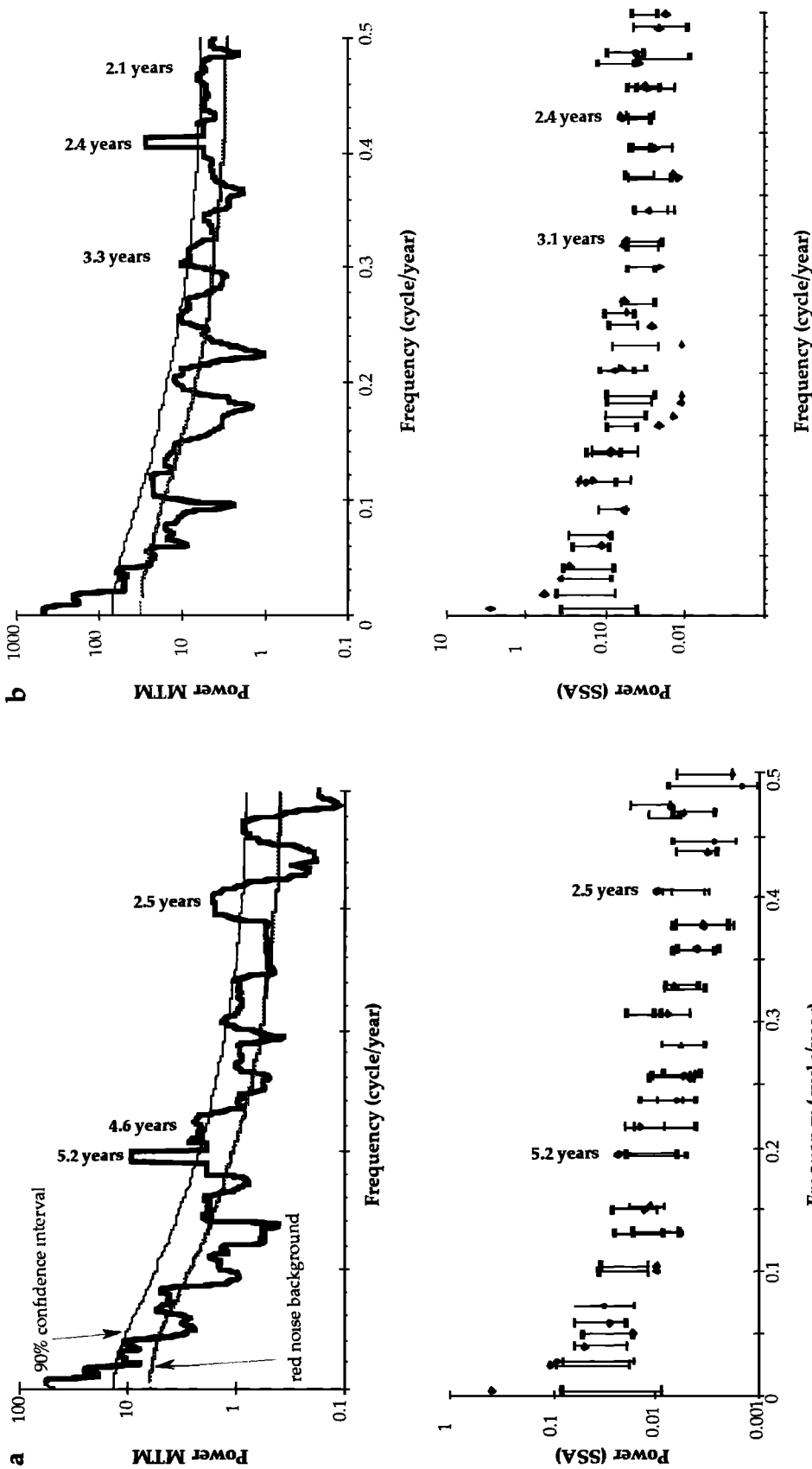

Figure 8. Multitaper method (MTM) and singular spectrum analysis (SSA) spectral analyses of (a) the annual $\delta^{18}O$ record and (b) the annual $\delta^{14}C$ signal. The top graphs show the power spectrum (thick line) of the time series. An estimate of the red noise background from a median smoothing is shown with continuous thin line. The dashed line represents a 90% confidence interval with respect to the red noise background. The lower graphs contains the SSA eigenvalue decomposition (vertical axis). The horizontal axis represents the frequency associated with each eigenvalue (through the corresponding eigenvector [*Allen and Smith*, 1996]. The confidence intervals are the 10% and 90% percentiles of Monte Carlo simulations of a red noise process that has the same statistical properties as the time series. Components that fall within the confidence intervals are thus statistically indistinguishable from red noise, whereas the red noise null hypothesis can be rejected when eigenvalues stand above the bars [*Allen and Smith*, 1996; *Yiou et al.*, 1996].

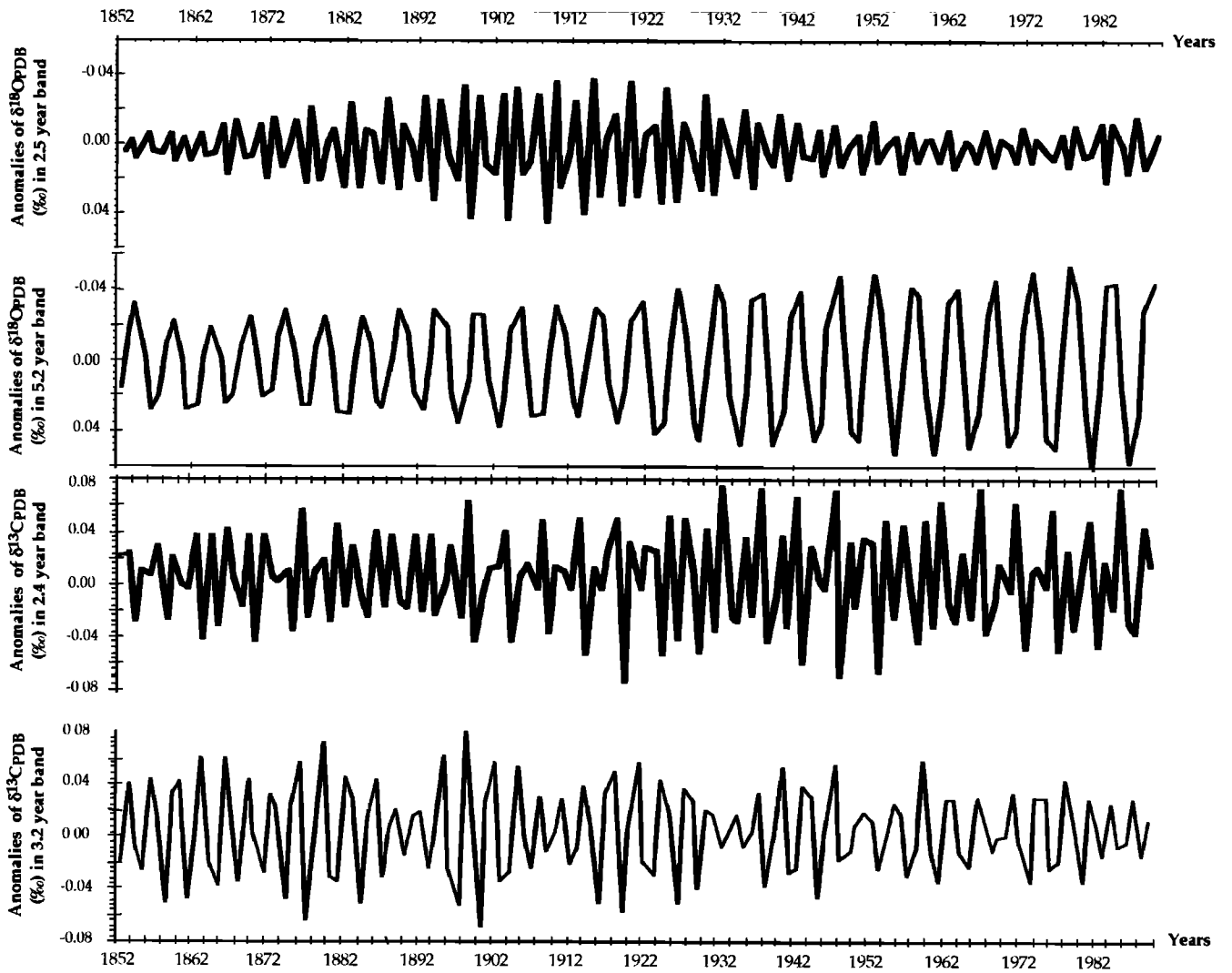

Figure 9. SSA decompositions of the Moorea coral $\delta^{18}O$ and $\delta^{13}C$ anomalies in 2 5 and 5.2 year bands and 2.5 and 3 2 year bands, respectively. These four climatic series show a strong variability over the past 137 years. From these four records an ENSO reconstruction was established taking into account each maximum of $\delta^{13}C$ anomaly in the (Y-1, Y) year followed by a minimum $\delta^{18}O$ anomaly in the (Y, Y+1) year; these two isotopic anomalies are associated to the ENSO event which was developped in the east equatorial Pacific in (Y, Y+1). For example (see Table 2), a maximum peak of $\delta^{13}C$ is observed in 1898-1899) followed by a minimum $\delta^{18}O$ anomaly in (1899-1900); these two isotopic anomalies are associated with the 1899-1900 event, which was a very strong ENSO [*Quinn*, 1992].

Niño detected from coral cores collected at Tarawa atoll [*Cole et al.*, 1993] and Galàpagos [*Druffel*, 1985]. Consequently, this temperature increase is probably caused by an ENSO event. While instrumental records from Tahiti do not show important anomalies associated with ENSO events, compared to the other areas of the equatorial Pacific Ocean [*Druffel*, 1985; *Cole et al.*, 1993], the spectral analysis of the two isotopic tracers from coral aragonite show typical ENSO periodicities.

5. Conclusion

Although Moorea is not located in a region where ENSO-associated anomalies are strong, the climatic variations in the south central Pacific Ocean strongly reflect the variability of the ENSO phenomenon since ~68% of ENSO events listed by both COADS and *Quinn* [1992] are registered by the Moorea climatology. Moreover, our ENSO reconstruction also shows that since the 1930s, few ENSO events have induced SST and precipitation anomalies in Moorea area.

Until now, $\delta^{18}O$ alone has been used as an ENSO indicator, recording temperature or $\delta^{18}O_{water}$ variations; herein $\delta^{13}C$ is used too as a powerful tracer. The present study calibrates the isotopic reconstruction over the past 33 years for which instrumental records allow a thorough comparison. It demonstrates the efficiency and the accuracy of a double tracer approach to reconstructing features of the oceanic and atmospheric variability during the past 137 years from the same coral core. By understanding the real significance of these two

Table 2. List of El Niño-Southern Oscillation (ENSO) Events Observed in both Annual $\delta^{13}C$ and $\delta^{18}O$ Records, *Quinn*'s Tabulation [1992], and the El Niño List From Comprehensive Oceanic-Atmospheric Data Set (COADS)

$\delta^{13}C$ Maximum Filtered in 3.2 Year Band	$\delta^{18}O$ Minimum Filtered in 2.5 Year Band	$\delta^{13}C$ Maximum Filtered in 3.2 Year Band	$\delta^{18}O$ Minimum Filtered in 5.2 Year Band	$\delta^{13}C$ Maximum Filtered in 2.4 Year Band	$\delta^{18}O$ Minimum Filtered in 5.2 Year Band	$\delta^{13}C$ Maximum Filtered in 2.4 Year Band	$\delta^{18}O$ Minimum Filtered in 2.5 Year Band	Our ENSO list	From Quinn [1992]	From COADS
		1853-1854	1854-1855	1853-1854	1854-1855			1854-1855	1854-1855	
1857-1858	1858-1859							1858-1859	1857-1859	
1859-1860	1860-1861					1859-1860	1860-1861	1860-1861	1860	
									1862	
									1864	
1864-1865	1865-1866							1865-1866	1865-1866	
1866-1867	1867-1868					1866-1867	1867-1868	1867-1868	1867-1869	
1869-1870	1870-1871					1869-1870	1870-1871	1870-1871	1871	
1871-1872	1872-1873							1872-1873	1873-1874	
1874-1875	1875-1876							1875-1876		
1876-1877	1877-1878							1877-1878	1876-1878	
1879-1880	1880-1881					1879-1880	1880-1881	1880-1881	1880-1881	
1881-1882	1882-1883							1882-1883		
1883-1884	1884-1885	1883-1884	1884-1885					1884-1885	1884-1885	
1886-1887	1887-1888					1886-1887	1887-1888	1887-1888	1887-1889	
1888-1889	1889-1890	1888-1889	1889-1890					1889-1890		
									1891	
1891-1892	1892-1893					1891-1892	1892-1893	1892-1893		
1893-1894	1894-1895	1893-1894	1894-1895					1894-1895		
1896-1897	1897-1898							1897-1898	1896-1897	
1898-1899	1899-1900	1898-1899	1899-1900	1898-1899	1899-1900	1898-1899	1899-1900	1899-1900	1899-1900	
									1901-1902	1902
1903-1904	1904-1905							1904-1905	1904-1905	1905
1906-1907	1907-1908							1907-1908	1907	
1908-1909	1909-1910					1908-1909	1909-1910	1909-1910		
						1911-1912	1912-1913	1912-1913	1911-1912	1911
1913-1914	1914-1915							1914-1915	1913-1915	1914
				1914-1915	1915-1916			1915-1916		
1918-1919	1919-1920					1918-1919	1919-1920	1919-1920	1918-1920	1918
		1920-1921	1921-1922					1921-1922		
						1921-1922	1922-1923	1922-1923	1923	1923
1923-1924	1924-1925							1924-1925		
1925-1926	1926-1927	1925-1926	1926-1927					1926-1927	1925-1926	1925
									1929-1931	1930
1930-1931	1931-1932	1930-1931	1931-1932	1930-1931	1931-1932	1930-1931	1931-1932	1931-1932	1932	1932
1935-1936	1936-1937							1936-1937		
									1939	1939
1940-1941	1941-1942					1940-1941	1941-1942	1941-1942	1940-1941	1941
						1943-1944	1944-1945	1944-1945	1943-1944	
									1951-1952	1951
		1951-1952	1952-1953	1951-1952	1952-1953			1952-1953	1953	1953
						1955-1956	1956-1957	1956-1957		
		1956-1957	1957-1958					1957-1958	1957-1958	1957
				1962-1963	1963-1964	1962-1963	1963-1964	1963-1964	1963-1964	
									1965-1966	1965
									1968-1969	1969
									1972-1973	1972
									1974-1975	
						1975-1976	1976-1977	1976-1977	1976-1977	1976
									1979-1980	
		1983-1984	1984-1985					1984-1985	1982-1983	1982-1983
1985-1986	1986-1987							1986-1987	1986-1987	1986

At Moorea, each ENSO event of the year (Y, Y+1) is characterized by an annual positive peak of $\delta^{13}C$ in (Y-1, Y) followed by an annual negative peak of $\delta^{18}O$ in (Y, Y+1) Thus, from singular-spectrum analysis decomposition records (see Figure 9), at this area an ENSO event can be characterized by. (1) either a $\delta^{13}C$ maximum filtered in 3.2 year band (column 1) which is followed by a $\delta^{18}O$ minimum filtered in 2 5 years (column 2), (2) a $\delta^{13}C$ maximum filtered in 3.2 year band (column 3) which is followed by a $\delta^{18}O$ minimum filtered in 5.2 years (column 4); (3) a $\delta^{13}C$ maximum filtered in 2.4 years (column 5) which is followed by a $\delta^{18}O$ minimum filtered in 5.2 years (column 6); or (4) a $\delta^{13}C$ maximum filtered in 2.4 years (column 7) which is followed by a $\delta^{18}O$ minimum filtered in 2.5 years (column 8). From these four lists we established a list of ENSO phenomena over the 1853-1989 period (column 9). These ENSO events (Y, Y+1) are compared to both *Quinn*'s [1992] tabulation (column 10) and the El Niño list from COADS (column 11)

proxies, in terms of meteorological change, we are able to estimate ENSO influence. During an ENSO year, oceanic temperature anomaly in the Moorea zone is always associated with changes of cloud cover; thus the annual $\delta^{13}C$ anomaly always precedes the annual $\delta^{18}O$ anomaly. Moreover, spectral analyses confirm that the observed isotopic anomalies exhibit typical ENSO periods, reflecting an ENSO influence at Moorea.

Acknowledgments. We especially thank D. Dole for assistance with the stable isotope measurements and M Stievenard for the measurements of oxygen isotopic composition of seawater The French National Meteorology Office and, particularly, F. Perrin (Faaa station, Tahiti) are gratefully acknowledged. We thank M. Pichon for the species determination of the coral core drilled in the Moorea lagoon. J.-P. Gattuso and L. Montaggioni provided insightful reviews of the manuscript. It is a pleasure to thank M Ghil and F Rougerie for discussions We also thank B. Chalker. M. Boiseau especially thanks La Societe de Secours des Amis de la Science. P Yiou is grateful to Michael Ghil for the sabbatical year he spent at IGPP, UCLA. Our thanks also go to the reviewers G. M Wellington and P. K. Swart This is LSCE contribution 71.

References

Allan, R J., The australasian summer monsoon, teleconnections, and flooding in the Lake Eyre Basin, Geogr. Rev Pap., *2*, 47, 1985

Allen, M. R, and L. A. Smith, Monte Carlo SSA: Detecting irregular oscillations in the presence of coloured noise, *J. Clim.*, *9*, 3373-3404, 1996.

Barnes, D J., and J. M Lough, On the nature and causes of density banding in massive coral skeletons, *J. Exp. Mar Biol. Ecol*, *167*, 91-108, 1993.

Barnes D. J , R. B Taylor and J. M Lough, On the inclusion of trace materials into massive coral skeletons, II, Distortions in skeletal records of annual climate cycles because of growth processes, *J Exp Mar Biol. Ecol*, *194*, 251-275, 1995.

Boiseau, M., and A. Juillet-Leclerc, H_2O_2 treatment of recent coral aragonite Oxygen and carbon isotopic implications, *Chem. Geol.*, *143*, 171-180, 1997

Carriquiry, J. D , M. J. Risk, and H P. Schwarcz, Stable isotope geochemistry of corals from Costa Rica as proxy indicator of the El Niño/Southern Oscillation (ENSO), *Geochim. Cosmochim. Acta*, *58*, 335-351, 1994

Cole, J E., and R. G Fairbanks, The Southern Oscillation recorded in the $\delta^{18}O$ of corals from Tarawa Atoll, *Paleoceanography*, *5*, 669-683, 1990.

Cole, J E., R G. Fairbanks, and G. T Shen, Recent variability in the Southern Oscillation: Isotopic results from a Tarawa Atoll coral, *Science*, *260*. 1790-1793, 1993

Dettinger, M. D., M. Ghil, C M Strong, W. Weibel, and P Yiou, Software expedites singular spectrum analysis of noisy time series, *Eos Trans. AGU*, *76*(2), 12, 14, 21, 1995.

Druffel, E R M , Detection of El Niño and decade time scale variations of sea surface temperature from banded coral records. implications for the carbon dioxyde cycle, in *The Carbon Cycle and Atmospheric CO_2: Natural Variations Archaen to Present*, Geophys. Monogr. Ser., vol. 32, edited by E T Sunquist and W.S. Broecker, pp. 111-121, Washington, D.C., 1985.

Dunbar, R. B., G. M Wellington, M. W. Colgan, and P W Glynn, Eastern Pacific sea surface temperature since 1600 A.D.: the $\delta^{18}O$ record of climate variability in Galàpagos corals, *Paleoceanography*, *9*, 291-315, 1994.

Epstein, S., R. Buchsbaum, H. Lowenstam, and H C Urey, Revised carbonate water isotopic temperature scale, *Geol Soc Am. Bull.*, *64*, 1315-1326, 1953.

Fairbanks, R G , and R E. Dodge, Annual periodicity of the $^{18}O/^{16}O$ and $^{13}C/^{12}C$ ratios in the coral *Monstastrea annularis*, *Geochim. Cosmochim. Acta*, *43*, 1009-1020, 1979.

Gagan, M. K , A. R. Chivas, and P. J Isdale, High resolution isotopic records from corals using ocean temperature and mass-spawing chronometers, *Earth Planeto. Sci Lett*, *121*, 549-558, 1994.

Ghil, M., and P Yiou, Spectral methods: What they can and cannot do for climatic time series, in *Decadal Climate Variability: Dynamics and Predictability*, edited by D. Anderson and J. Willebrand, pp. 445-481, Elsevier, New York, 1996

Goreau, T J., Coral skeletal chemistry physiological and environmental regulation of stable isotope and trace metals in *Montastrea annularis*, *Proc R. Soc London, Ser. B 196*, 291-315, 1977.

Grossman, E L , and T L. Ku, Oxygen and carbon isotope fractionation in biogenic aragonite: Temperature effects, *Chem. Geol.*, *59*, 59-74, 1986.

Ivanoff, A., Introduction à l'océanographie (propriétés physiques et chimiques des eaux de mer), Collection de l'Enseignement à la Recherche Océanographique, tome II, Vuibert, Paris, 1975

Jiang, N., J D. Neelin, and M. Ghil, Quasi-quadrennal and quasi-biennal variability in the equatorial Pacific, *Clim. Dyn.*, *12*, 101-112, 1995

Jin, F. F , J. D. Neelin, and M. Ghil, El Niño on the Devil's staircase Annual subharmonic steps to chaos, *Science*, *264*, 70-72,1994

Juillet-Leclerc, A., J. P. Gattuso, L. F. Montaggioni, and M. Pichon, Seasonal variation in primary productivity and in the skeletal $\delta^{13}C$ and $\delta^{18}O$ in the reef-buiding scleractinian coral *Acropora formosa*, *Mar. Ecol. Prog. Ser.*, *157*, 109-117, 1997.

Kirk, J T O , *Light and Photosynthesis in Aquatic Ecosystems*, 401 pp., Cambridge Univ. Press, New York, 1983.

Leder, J J., P. K. Swart, A. M. Szmant, and R. E. Dodge, The origin of variations in the isotopic record of scleractinian corals, I, Oxygen, *Geochim. Cosmochim. Acta*, *60*, 2857-2870, 1996.

McConnaughey, T., ^{13}C and ^{18}O isotopic disequilibrium in biological carbonates, I, Patterns, *Geochem. Cosmochim. Acta*, *53*, 151-162, 1989

Philander, S. G., *El Niño, la Niña, and the Southern Oscillation*, Int. Geophys. Ser., vol 46, edited by R. Dmowska and J. R. Holton, 293 pp , Academic, San Diego, California, 1989.

Quinn, T. M., F. W. Taylor, and T. J. Crowley, A 173 year stable isotope record from a tropical south Pacific coral, *Quat. Sci. Rev.*, *12*, 407-418, 1993

Quinn, T. M., F. W. Taylor, T. J. Crowley, and S. M. Link, Evaluation of sampling resolution in coral stable isotope records: A case study using records from New Caledonia and Tarawa, *PaleOceanography*, *11*, 529-542, 1996.

Quinn, W. H, A study of Southern Oscillation related climatic activity for A.D. 622-1900 incorporating Nile river flood data, in *El Niño: Historical and Paleoclimatic Aspects of the Southern Oscillation*, edited by H F. Diaz and V. Markgraph, pp. 119-149, Cambridge Univ. Press, New York, 1992.

Rasmusson, E. M., X. Wang, and C. F Ropelewski, The biennal component of ENSO variability, *J. Mar Syst.*, *1*, 71-96, 1990.

Rougerie, F., L. Marec, and B. Wauthy, Caractéristiques hydroclimatiques de la zone marine polynésienne en 1982 et 1983, *ORSTOM Tahiti Notes et Doc Océanogr.*, *27*, 112, 1985.

Swart, P. K., Carbon and oxygen isotope fractionation in scleractinian corals: A review, *Earth Sci Rev.*, *19*, 51-80, 1983

Swart, P K., J. J Leder, A M. Szmant, and R E Dodge, The origin of variations in the isotopic record of scleractinian corals, II, Carbon, *Geochim. Cosmochim Acta*, *60*, 2871-2886, 1996.

Tarutani, T , R. N. Clayton, and T K Mayeda, The effect of polymorphism and magnesium substitution on oxygen isotope fractionation between calcium carbonate and water, *Geochim. Cosmochim. Acta*, *33*, 987-996, 1969.

Thomson, D. J , Spectrum estimation and harmonic analysis, *Proc IEEE*, *9*, 1055-1096, 1982

Tziperman, E., L. Stone, M A. Cane, and H. Jarosh, El Niño chaos: Overlapping of resonances between the seasonal cycle and the Pacific Ocean-atmosphere oscillator, *Science*, *264*, 72-74, 1994.

Vautard, R., and M Ghil, Singular spectrum analysis in nonlinear dynamics, with applications to paleoclimatic time series, *Physica D*, *35*, 395-424, 1989.

Weber, J N , and P. M. J. Woodhead, Diurnal variations in the isotopic composition of dissolved inorganic carbon in seawater from coral reef environments, *Geochim. Cosmochim. Acta*, *35*, 891-902, 1971.

Wellington, G. M., R. B Dunbar, and G. Merlen, Calibration of stable oxygen isotope signatures in Galàpagos corals, *Paleoceanography*, *11*, 467-480, 1996.

Yiou, P., M. F. Loutre, and E. Baert, Spectral analysis of climate data, *Surv. Geophys.*, *17*, 619-663, 1996.

M. Boiseau, Institute of Geophysics and Planetary Physics, University of California, 405 Hilgard avenue, Los Angeles, CA 90095-1567 (Muriel.Boiseau@atmos.ucla.edu)

M. Guillaume, Laboratoire de Biologie des Invertébrés Marins, Museum National d'Histoire Naturelle, 75231 Paris, France.

P Isdale, Australian Institute of Marine Science, PMB n°3, Townsville, Queensland 4810, Australia.

A. Juillet-Leclerc and P. Yiou, Laboratoire des Sciences du Climat et de l'Environnement, Laboratoire mixte CNRS-CEA, 91180 Gif-sur-Yvette Cedex, France.

J. Salvat, Laboratoire de Biologie Marine, EPHE, URA-CNRS 1453, Université de Perpignan, 66860 Perpignan Cedex, France.

(Received October 30, 1997;
revised July 9, 1998;
accepted July 13, 1998)